European Radiology (2019) 29:2553–2559
https://doi.org/10.1007/s00330-018-5859-3

CONTRAST MEDIA

Gadolinium-enhanced imaging of pediatric thoracic lymphoma: is intravenous contrast really necessary?

Christophe T. Arendt[1] · Martin Beeres[1] · Doris Leithner[1] · Patricia Tischendorf[1] · Marcel Langenbach[1] · Benjamin Kaltenbach[1] · Jasmin Dalgicdir[1] · Thomas J. Vogl[1] · Tatjana Gruber-Rouh[1]

Received: 31 July 2018 / Revised: 27 September 2018 / Accepted: 25 October 2018 / Published online: 13 December 2018

Abstract

Objectives Increasing awareness of potential side effects from gadolinium-based contrast agents has underlined the need for contrast-free magnetic resonance imaging (MRI). Numerous recent articles evaluated the risk of potential brain deposits, with the result that research is putting the focus more on alternative unenhanced imaging techniques. The aim of this study was to determine the need for contrast media for chest MRI in primary staging and follow-up care of lymphoma.

Methods This monocentric, retrospective study encompassed patients under 25 years of age who had undergone histopathological examination of thoracic lymph nodes and at least one chest MRI examination with unenhanced and contrast-enhanced sequences. Seven different thoracic lymph node stations including mediastinal, hilar, periclavicular, and axillary regions were evaluated by two readers regarding lesion diameter, number, shape, necrosis, and infiltration of surrounding structures. Findings were categorized into suspicious (> 1 cm; round; necrosis; infiltration) or non-suspicious.

Results Fifty-one patients (mean age, 16.0 ± 3.7 yrs) with thoracic Hodgkin (70.6%) and non-Hodgkin lymphoma (25.5%) and lymphadenopathy (3.9%) were retrospectively included. Most lymph nodes categorized as suspicious were located in the mediastinal station (86.4%). High agreement ($\kappa = 0.81$) between unenhanced and contrast-enhanced sequences was found for both suspicious and non-suspicious lymph nodes. Significant ($p < 0.001$), but small difference (1 mm) was observed only in sizing mediastinal lymph nodes (all other $p > 0.05$). No significant difference (smallest $p = 0.08$) was shown for the use of five different types of contrast media.

Conclusion MRI in young patients with thoracic lymphoma can safely be done without the use of contrast agent.

Key Point

- *Thoracic magnetic resonance imaging in young lymphoma patients can safely be done without gadolinium-based contrast agents.*

Keywords Lymphoma · Magnetic resonance imaging · Contrast media · Pediatrics

Abbreviations

ADC	Apparent diffusion coefficient
DWI	Diffusion-weighted imaging
FDG-PET/CT	Fluorodeoxyglucose-positron emission tomography/computed tomography
GBCA	Gadolinium-based contrast agent
HL	Hodgkin lymphoma
MRI	Magnetic resonance imaging
NHL	Non-Hodgkin lymphoma

✉ Christophe T. Arendt
crt.arendt@gmail.com

[1] Department of Diagnostic and Interventional Radiology, University Hospital Frankfurt, Theodor-Stern-Kai 7, 60590 Frankfurt/Main, Germany

Introduction

Therapeutic advances in Hodgkin (HL) and non-Hodgkin lymphoma (NHL), which account for two of the most frequent childhood malignancies, have led to an increasing survival rate of young patients [1]. Follow-up care with radiological imaging in a growing population of cancer-survivors is therefore of paramount importance. For disease staging, treatment planning, and initial response to therapy, whole-body fluorodeoxyglucose-positron emission tomography/computed

tomography (FDG-PET/CT) is considered the current reference imaging method [2, 3]. However, this examination is accompanied by substantial radiation dose and cancer risk [4], along with the fact that children are more sensitive to the risks of ionizing radiation and have a longer post-exposure life expectancy to exhibit long-term effects [5]. Whole-body magnetic resonance imaging (MRI) may be a valuable alternative [6–8] and is radiation-free, but there is very little data comparing unenhanced and contrast-enhanced chest MRI for pediatric thoracic lymphoma.

In general, contrast-enhanced MRI examinations are very well tolerated by the majority of patients because adverse effects to gadolinium-based contrast agents (GBCA), such as allergic-like reactions and kidney disorders, are rare [9]. Nevertheless, the use of GBCA has fallen into disrepute since Kanda et al postulated that remnants of gadolinium may be deposited in the dentate nucleus and the globus pallidus [10]. Those findings were also observed in the brain of children with repeated exposure to linear GBCA [11, 12]. By contrast, multiple research groups have underlined that macrocyclic agents, with their cage-like ligand structure, seem to be safer [13–16]. Many pediatric hospitals in North America [17] and Europe have switched from linear to macrocyclic GBCA as a consequence. Thus, radiologists and referring physicians are obliged to pay even more specific attention to the newer safety concerns, and GBCA, both linear and macrocyclic, should not be used if they are not absolutely needed.

We therefore designed a retrospective radiologic-pediatric study in a patient cohort suffering from thoracic HL, NHL, or lymphadenopathy to determine whether there is any significant difference between unenhanced and contrast-enhanced MRI in terms of (1) categorization of lymph nodes into suspicious and non-suspicious, and (2) size and (3) number of suspicious lymph nodes.

Materials and methods

Patient selection

The institutional review board approved the research protocol of this retrospective monocentric study and waived the need for informed patient consent. All procedures were carried out in accordance with the Declaration of Helsinki (2000).

Our study enrolled patients under 25 years of age who underwent both an initial histopathological analysis of suspicious thoracic lymph nodes and at least one chest MRI with unenhanced and contrast-enhanced sequences. Lymphoma subtypes were diagnosed based on tissue samples obtained by biopsy or surgery. All MRI studies between January 2010 and October 2016 were consecutively included. Examinations without intravenous administration of GBCA, premature termination due to claustrophobia, and patients older than mentioned above were excluded.

Image acquisition and contrast media

All images were acquired on a 3 Tesla MRI scanner (MAGNETOM Prisma, Siemens Healthineers). Patients were positioned head-first in a supine position and the chest was covered with an 18-channel phased-array body coil. Spine coil elements in the patient table were switched on. Standard imaging protocol with unenhanced and contrast-enhanced sequences is described in Table 1. Sequences were acquired during multiple end-expiratory breath holds. Contrast medium was injected with a flow rate of 1 ml/s and the amount was contingent upon patient's body weight and the recommended dose from the selected vendor, respectively. Time points of the follow-up MRI investigations were dependent on the histological type of lymphoma and the clinical course of the respective patient.

Five different types of GBCA were utilized during the relevant time period, including (1) gadobutrol (Gadovist, Bayer Vital GmbH), (2) gadoteric acid (Dotarem, Guerbet GmbH), (3) gadoteridol (ProHance, Bracco Diagnostics Inc.), (4) gadobenate dimeglumine (MultiHance, Bracco Diagnostics Inc.), and (5) gadopentetate dimeglumine (Magnevist, Bayer HealthCare Pharmaceuticals). The latter two GBCA have a linear molecular geometry, while the other mentioned GBCA are macrocyclic.

Table 1 Standard imaging protocol of chest MRI scans

Unenhanced MRI sequences	Contrast-enhanced MRI sequences
T1-fl2d[a] (tra[b])	T1-fl2d-fs[c] (tra)
T1-vibe[d]-fs (tra)	T1-vibe-fs (tra)
T1-vibe-dixon-caipirinha[e]-in/opp/F/W[f] (tra)	T1-vibe-dixon-caipirinha-in/opp/F/W (tra)
T2-HASTE[g] (tra/cor[h])	
ep2D[i]-diff[j]-b50-b800-TRACE (tra)	
ep2D-diff-b50-b800-ADC[k] (tra)	

MRI magnetic resonance imaging

[a] Two-dimensional fast low angle shot

[b] Transverse

[c] Fat saturation

[d] Volumetric interpolated breath-hold examination

[e] Controlled aliasing in parallel imaging results in higher acceleration

[f] In phase/opposed phase/fat/water

[g] Half-Fourier acquisition single-shot turbo spin echo

[h] Coronal

[i] Two-dimensional echo-planar

[j] Diffusion-weighted

[k] Apparent diffusion coefficient

Image interpretation

All datasets were evaluated directly on the picture archiving and communication system (GE Centricity PACS, GE Healthcare). Image analysis was independently performed by two raters, the first one with more than 1 year of experience in MRI interpretation and the second one with more than 8 years of experience including pediatric expert knowledge. The examinations were split up among both raters. All images were rated twice with a minimal time interval of 2 weeks, firstly in alphabetical and secondly in random order. Each rater could individually regulate the window levels of the images. Both readers were informed about the patient's medical history.

Both raters evaluated images of unenhanced T1-weighted sequences with and without fat suppression, unenhanced T2-weighted sequences, DWI-sequences with ADC map, where available, and contrast-enhanced T1-weighted sequences with fat suppression. On the whole, seven different thoracic lymph node stations were analyzed, including mediastinal, right and left axillary, right and left periclavicular, and right and left hilar region. In each station, the largest lymph node(s) visualized was assessed regarding (a) lesion diameter, (b) shape, (c) presence of intralesional necrosis, (d) contrast enhancement, and (e) infiltration of surrounding structures. Presence of (f) bulky disease, defined as a maximal diameter more than 7 cm or more than one third of the mediastinal mass ratio [18], was also indicated. Diameters of lymph nodes and lymphoma were measured on T1-weighted images. Furthermore, (g) the number of suspicious lymph nodes in the respective lymph node group was determined. Findings were categorized into suspicious (lesion diameter > 10 mm, round shape with a short-to-long-axis ratio greater than 0.5, necrosis, marked contrast enhancement, infiltrative growth) or non-suspicious (≤ 10 mm, elliptical with a short-to-long-axis ratio less than 0.5, no necrosis, no or low enhancement, no infiltration). Restricted diffusion, defined as high signal on b800-DWI images with low signal on corresponding ADC map, was considered to be pathological. Only lymph nodes with a diameter of ≥ 3 mm were included and measured.

Statistical analysis

Descriptive statistical data was provided as counts and proportions or mean values with single standard deviation and ranges. Kolmogorov-Smirnov test with Lillifors correction was used to test the data for normal distribution. Cohen's Kappa Coefficient (κ) was used as a measure of agreement between unenhanced and contrast-enhanced sequences for the categorization of the largest lymph node into suspicious and non-suspicious, and for the number of suspicious lymph nodes in each thoracic lymph node station. We considered rates of agreement as follows: $\kappa < 0$, poor; $\kappa = 0.0$–0.20, slight; $\kappa = 0.21$–0.40, fair; $\kappa = 0.41$–0.60, moderate; $\kappa = 0.61$–0.80, substantial; $\kappa = 0.81$–1.0, (almost) perfect [19]. The Wilcoxon signed-rank test was calculated to compare the size of the respective largest lymph node between MRI sequences with and without contrast agent. The Kruskal-Wallis test was applied for comparing the various types of GBCA with regard to the above mentioned analyses. Significance was accepted for p values < 0.05. All computations were performed using BiAs, version 11.8 (epsilon Verlag).

Results

Patient characteristics

This retrospective, monocentric study analyzed a total of 51 patients, 20 (39.2%) female and 31 (60.8%) male, with an average age of 16.0 ± 3.7 years (age range, 4–23 years). All patients underwent histological examination of at least one suspicious thoracic lymph node, with HL in 36 (70.6%), NHL in 13 (25.5%), and lymphadenopathy in 2 (3.9%) cases. Regarding the latter, one patient was diagnosed with T cell acute lymphoblastic leukemia during follow-up care and the second case was interpreted as generalized lymphadenopathy of unknown origin. In total, 236 chest MRI examinations were analyzed, as 36 patients (70.6%) received at least one follow-up MRI, with an average number of 4.7 ± 3.5 (range, 1–15) per patient.

Comparison between unenhanced and enhanced MRI sequences

Most lymph nodes categorized as suspicious were located in the mediastinal region ($n = 204/236$, 86.4%). Moreover, in descending order, further suspicious lymph nodes were detected in left periclavicular ($n = 54/236$, 22.9%), right periclavicular ($n = 40/236$, 16.9%), left axillary ($n = 34/236$, 14.4%), right hilar (18/236, 7.6%), right axillary ($n = 13/236$, 5.5%), and left hilar ($n = 13/236$, 5.5%) region. There was almost perfect agreement between unenhanced and contrast-enhanced-sequences for the categorization of the largest lymph node into both suspicious and non-suspicious, with lowest $\kappa = 0.88$ overall.

In addition, perfect agreement ($\kappa = 1$) between sequences with and without GBCA was observed for the number of suspicious lymph nodes in each thoracic lymph node station. The results were as follows: mediastinal, 1.4 ± 0.9 (range, 0–4), right axillary, 0.1 ± 0.3 (0–3); left axillary, 0.3 ± 0.8 (0–8); right periclavicular, 0.2 ± 0.4 (0–3); left periclavicular, 0.3 ± 0.5 (0–3); right hilar, 0.1 ± 0.3 (0–1); and left hilar region, 0.1 ± 0.3 (0–2).

Furthermore, Wilcoxon matched-pairs-test showed a significant ($p < 0.001$), but small difference of 1 mm for the

sizing of the largest lymph node in the respective mediastinal lymph node station. No significant difference in sizing lymph nodes was found in the other six regions (all $p > 0.05$). Largest lymph nodes were measured in the mediastinum, with an average size of 19.0 ± 11.0 mm (5–86 mm). Further lesion sizes were as follows: right axillary, 6.7 ± 1.9 mm (3–16 mm); left axillary, 7.1 ± 3.8 mm (3–29 mm); right periclavicular, 9.7 ± 5.0 mm (3–28 mm); left periclavicular, 10.2 ± 5.4 mm (3–30 mm); right hilar, 13.7 ± 9.1 mm (4–40 mm); and left hilar region, 13.5 ± 4.0 mm (5–26 mm). Fourteen patients (27.5%) suffered initially from bulky disease, and all of them showed therapeutic response with shrinkage of their tumors during follow-up care.

Figure 1 demonstrates a Bland-Altman plot with significantly different lesion sizes in the mediastinal nodal station between contrast-enhanced and unenhanced sequences. A representative case of a study participant is shown in Fig. 2.

Contrast agent

Dotarem was the most often administered GBCA during this study, with $n = 130$ (55.1%). The other two macrocyclic GBCA, Gadovist and ProHance, were utilized in 80 (33.9%) and 14 (5.9%) cases, respectively. Linear GBCA were only used at the beginning of the study time period, with $n = 9$ (3.8%) for MultiHance and $n = 3$ (1.3%) for Magnevist. In each thoracic lymph node station, no statistical significance was observed regarding size measurement (lowest $p = 0.24$, in left periclavicular station) and number of suspicious lymph nodes (lowest $p = 0.08$, in right periclavicular station) in contrast-enhanced sequences. Furthermore, differences in size measurement of lymph nodes between unenhanced and contrast-enhanced sequences were not statistically significant (lowest $p = 0.12$, in left periclavicular station). All p values are presented in Table 2.

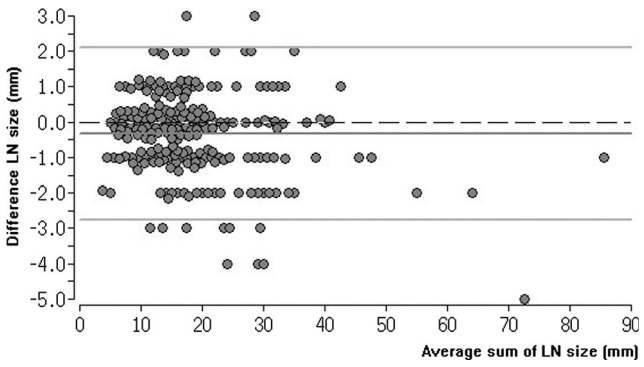

Fig. 1 Agreement between unenhanced and contrast-enhanced MRI for sizing mediastinal lymphoma. This Bland-Altman plots shows a significant ($p < 0.001$) but small (1 mm) difference for the assessment of lesion size in the mediastinal lymph node station

Discussion

In this cohort of children and adolescents being investigated for thoracic HL, NHL, or lymphadenopathy, the intravenous administration of GBCA in chest MRI was not necessarily required (1) to categorize lymph nodes into suspicious and non-suspicious, and (2) to measure and (3) to count suspicious lymph nodes in all thoracic nodal stations. Both observers with different expertise levels were highly confident throughout the analyses, showing high concordance between unenhanced and contrast-enhanced sequences for the endpoints. Furthermore, the chosen type of macrocyclic or linear GBCA did not significantly affect the results.

There have been a few previous studies which investigated the impact of contrast-free inversion recovery [6] and diffusion-weighted [7, 8] sequences for the initial whole-body staging of pediatric lymphoma. Mayerhoefer and co-workers highlight the important role of DWI-MRI in the largest patient cohort with regard to follow-up care and treatment response assessment of lymphoma [20]. Their results underline that unenhanced MRI may serve as a good radiation-free alternative to FDG-PET/CT. A more recent study has shown that FDG-PET/MRI with additional DWI-sequence may even surpass FDG-PET/CT, particularly in indolent NHL [21]. However, PET/MRI is currently not a widely used examination due to its limited availability and some remaining technical issues. In the present study, we therefore focused on the relevance of unenhanced chest MRI for the follow-up of young lymphoma patients without extrathoracic manifestations. In general, chest MRI in the evaluation of cardiothoracic lymphoma is also useful to assess involvement of chest wall, heart, and vessels [22].

Our results indicate that the repetitive use of contrast media at multiple time points during follow-up care may not be necessary to improve the diagnostic value. As remnants of linear GBCA have been indirectly detected in the brain of children [11, 12], unenhanced examinations should take precedence over contrast-enhanced MRI. In addition, adverse effects (e.g., allergic-like reactions, acute and chronic kidney disorders, nephrogenic systemic fibrosis, and other effects as yet unknown) could be avoided. In addition to the invasive insertion of a venous cannula for the administration of GBCA, prolonged examination times are stressful and may result in premature termination of the MRI. Moreover, the administration of intravenous contrast may result in sedation or general anesthesia being needed—which is not without risks, and requires a dedicated anesthetics team and an established safe environment in the department of radiology [23].

Our standard imaging protocol included latest state-of-the-art sequences on a 3 Tesla scanner. Both raters used T1-weighted images for size measurement of the lesions, as partial volume effects may be significant in DWI-MRI [24]. Regarding the latter, optimal b values have not yet been suggested for the thorax. However, these should be greater than

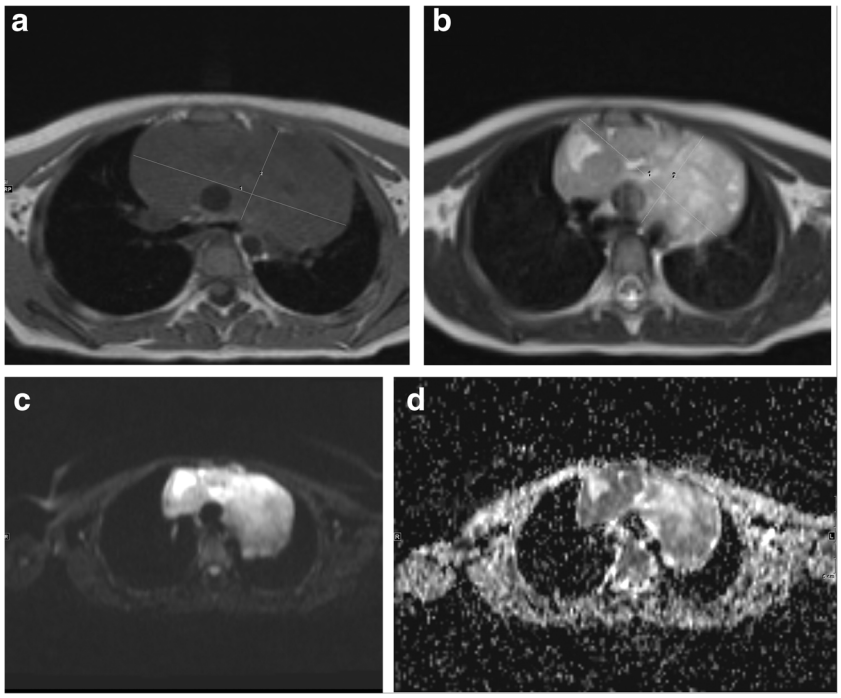

Fig. 2 Representative case. 6-year-old girl with bulky mediastinal T cell lymphoma. **a** Unenhanced and (**b**) contrast-enhanced MRI images (T1-fl2d) reveal a lesion size of 96.2 × 45.2 mm and 96.5 × 44.6 mm, respectively. **c** DWI-MRI with (**d**) corresponding ADC map show a pathologically restricted diffusion, with high signal on high *b* value and low signal on calculated map

500 s/mm^2 to avoid the effects of perfusion and less than 1000 s/mm^2 for a better signal-to-noise ratio [25, 26]. Similar to the study of Giraudo et al [21], our imaging protocol included DWI-MRI with a *b* value of 800 s/mm^2 and, additionally, with a value of 50 s/mm^2 for the calculation of the ADC map. On the other hand, most research groups used a *b* value of 1000 s/mm^2 for chest MRI to better assess the lung parenchyma in the setting of lung tumors [26].

Notably, lesion diameters differed significantly in the mediastinal node station but not in all other regions. There are different possible explanations for this discrepancy: (1) the largest lymph nodes and most of the bulky diseases were located in the mediastinum, which can lead to higher measurement uncertainty; (2) contrast-enhanced images were acquired at the end of the examination, with possible occurrence of motion artifacts or reduced patient compliance with regard to the breathing commands. Moreover, the size difference of solely 1 mm has no relevant clinical impact. Furthermore, MRI of the chest has a higher spatial resolution in comparison to whole-body MRI studies due to lower field of view, which should result in higher measurement accuracy.

Some limitations have to be taken into account. First, the present study is monocentric and retrospective, and further prospective investigations may be necessary to support our results. Second, we did not carry out a large cohort study; however, our study population was heterogeneous regarding age, gender, histological subtype, treatment regime, and clinical course. Third, the field of view of the MRI was limited to the chest and further extrathoracic lymph node groups could not be evaluated. Yet, our study results could be transferred to other body regions, such as the neck and the groin, based on the typical imaging characteristics of lymphoma. HL and NHL although comprise an inhomogeneous group of neoplasm including many subtypes, and therefore, fourth, a dedicated

Table 2 Results of Kruskal-Wallis tests to compare five different types of GBCA regarding (A) size difference of suspicious lymph nodes between unenhanced and contrast-enhanced sequences, and (B) number and (C) size of suspicious lymph nodes in contrast-enhanced sequences

	(A) Significance (*p* value)	(B) Significance (*p* value)	(C) Significance (*p* value)
Mediastinal LNS[a]	0.96	0.72	0.53
Right axillary LNS	0.20	0.16	0.54
Left axillary LNS	0.85	0.52	0.55
Right periclavicular LNS	0.97	0.08	0.97
Left periclavicular LNS	0.12	0.21	0.24
Right hilar LNS	0.43	0.70	1.00
Left hilar LNS	0.24	0.06	0.69

GBCA gadolinium-based contrast agents

[a] Lymph node station

subtype analysis would have been preferable. Fifth, the examinations were conducted solely on a 3 Tesla scanner, with known superior image quality to images obtained from lower magnetic field strength due to improved signal-to-noise-ratio and resolution. Sixth, we only considered histology as the main reference standard and did not take initial imaging findings of FDG-PET/CT into account. However, diagnostic performance of MRI against this reference imaging method has already been evaluated [6–8, 20], and our study focused on the comparison between unenhanced and contrast-enhanced MRI.

In conclusion, this radiological study in a pediatric and adolescent cohort highlights the need to raise awareness of unnecessary intravenous administration of GBCA in follow-up chest MRI for the imaging of thoracic lymphoma and lymphadenopathy. Therefore, we suggest that radiologists and referring physicians should at least consider to not give additional contrast, on condition that breath-hold T1-, T2-, and diffusion-weighted sequences are included in the standard imaging protocol.

Funding information The authors state that this work has not received any funding.

Compliance with ethical standards

Guarantor The scientific guarantor of this publication is Prof. Dr. Thomas J. Vogl, Head of the Department of Interventional and Diagnostic Radiology, University Hospital Frankfurt.

Conflict of interest The authors of this manuscript declare no relationships with any companies, whose products or services may be related to the subject matter of the article.

Statistics and biometry Prof. Dr. Eva Herrmann, Head of the Institute of Biostatistics and Mathematic Modeling, University Hospital Frankfurt, kindly provided statistical advice for this manuscript.

Informed consent Written informed consent was waived by the Institutional Review Board.

Ethical approval Institutional Review Board approval was obtained.

Methodology
- retrospective
- not applicable
- performed at one institution

References

1. Buhtoiarov IN (2017) Pediatric lymphoma. Pediatr Rev 38:410–423
2. Cheson BD, Fisher RI, Barrington SF et al (2014) Recommendations for initial evaluation, staging, and response assessment of Hodgkin and non-Hodgkin lymphoma: the Lugano classification. J Clin Oncol 32:3059–3068
3. Johnson SA, Kumar A, Matasar MJ, Schöder H, Rademaker J (2015) Imaging for staging and response assessment in lymphoma. Radiology 276:323–338
4. Huang B, Law MW, Khong PL (2009) Whole-body PET/CT scanning: estimation of radiation dose and cancer risk. Radiology 251:166–174
5. Kutanzi KR, Lumen A, Koturbash I, Miousse IR (2016) Pediatric exposures to ionizing radiation: carcinogenic considerations. Int J Environ Res Public Health 13(11):1057. https://doi.org/10.3390/ijerph13111057
6. Punwani S, Taylor SA, Bainbridge A et al (2010) Pediatric and adolescent lymphoma: comparison of whole-body STIR half-Fourier RARE MR imaging with an enhanced PET/CT reference for initial staging. Radiology 255:182–190
7. Kwee TC, van Ufford HM, Beek FJ et al (2009) Whole-body MRI, including diffusion-weighted imaging, for the initial staging of malignant lymphoma: comparison to computed tomography. Invest Radiol 44:683–690
8. Littooij AS, Kwee TC, Barber I et al (2014) Whole-body MRI for initial staging of paediatric lymphoma: prospective comparison to an FDG-PET/CT-based reference standard. Eur Radiol 24:1153–1165
9. American College of Radiology (2017) ACR manual on contrast media version 10.3. Available via https://www.acr.org/Clinical-Resources/Contrast-Manual. Accessed 03 Jan 2018
10. Kanda T, Ishii K, Kawaguchi H, Kitajima K, Takenaka D (2014) High signal intensity in the dentate nucleus and globus pallidus on unenhanced T1-weighted MR images: relationship with increasing cumulative dose of a gadolinium-based contrast material. Radiology 270:834–841
11. Flood TF, Stence NV, Maloney JA, Mirsky DM (2017) Pediatric brain: repeated exposure to linear gadolinium-based contrast material is associated with increased signal intensity at unenhanced T1-weighted MR imaging. Radiology 282:222–228
12. Hu HH, Pokorney A, Towbin RB, Miller JH (2016) Increased signal intensities in the dentate nucleus and globus pallidus on unenhanced T1-weighted images: evidence in children undergoing multiple gadolinium MRI exams. Pediatr Radiol 46:1590–1598
13. Radbruch A, Weberling LD, Kieslich PJ et al (2015) Gadolinium retention in the dentate nucleus and globus pallidus is dependent on the class of contrast agent. Radiology 275:783–791
14. Radbruch A, Haase R, Kickingereder P et al (2017) Pediatric brain: no increased signal intensity in the dentate nucleus on unenhanced T1-weighted MR images after consecutive exposure to a macrocyclic gadolinium-based contrast agent. Radiology 283:828–836
15. Bae S, Lee HJ, Han K et al (2017) Gadolinium deposition in the brain: association with various GBCAs using a generalized additive model. Eur Radiol 27:3353–3361
16. Kanda T, Osawa M, Oba H et al (2015) High signal intensity in dentate nucleus on unenhanced T1-weighted MR images: association with linear versus macrocyclic gadolinium chelate administration. Radiology 275:803–809
17. Mithal LB, Patel PS, Mithal D, Palac HL, Rozenfeld MN (2017) Use of gadolinium-based magnetic resonance imaging contrast agents and awareness of brain gadolinium deposition among pediatric providers in North America. Pediatr Radiol 47:657–664
18. Kumar A, Burger IA, Zhang Z et al (2016) Definition of bulky disease in early stage Hodgkin lymphoma in computed tomography era: prognostic significance of measurements in the coronal and transverse planes. Haematologica 101:1237–1243
19. Landis JR, Koch GG (1977) The measurement of observer agreement for categorical data. Biometrics 33:159–174
20. Mayerhoefer ME, Karanikas G, Kletter K et al (2015) Evaluation of diffusion-weighted magnetic resonance imaging for follow-up and treatment response assessment of lymphoma: results of an 18F-FDG-PET/CT-controlled prospective study in 64 patients. Clin Cancer Res 21:2506–2513

21. Giraudo C, Raderer M, Karanikas G et al (2016) 18F-fluorodeoxyglucose positron emission tomography/magnetic resonance in lymphoma: comparison with 18F-fluorodeoxyglucose positron emission tomography/computed tomography and with the addition of magnetic resonance diffusion-weighted imaging. Invest Radiol 51:163–169
22. Carter BW, Wu CC, Khorashadi L et al (2014) Multimodality imaging of cardiothoracic lymphoma. Eur J Radiol 83:1470–1482
23. Arlachov Y, Ganatra RH (2012) Sedation/anaesthesia in paediatric radiology. Br J Radiol 85:e1018–e1031
24. Alexander AL, Hasan KM, Lazar M, Tsuruda JS, Parker DL (2001) Analysis of partial volume effects in diffusion-tensor MRI. Magn Reson Med 45:770–780
25. Razek AA (2012) Diffusion magnetic resonance imaging of chest tumors. Cancer Imaging 12:452–463
26. Henzler T, Schmid-Bindert G, Schoenberg SO, Fink C (2010) Diffusion and perfusion MRI of the lung and mediastinum. Eur J Radiol 76:329–336